

# Decreased substrate affinity upon alteration of the substrate-docking region in cytochrome P450<sub>BM-3</sub>

Shelley A. Maves, Hyeyeong Yeom<sup>1</sup>, Mark A. McLean, Stephen G. Sligar\*

Beckman Institute for Advanced Science and Technology and Department of Biochemistry, University of Illinois, 405 N. Mathews Avenue, Urbana, IL 61801, USA

Received 19 June 1997; revised version received 28 July 1997

**Abstract** A mutation at the surface of the substrate access channel which dramatically decreases the affinity for some fatty acids in P450<sub>BM-3</sub> was discovered by random mutagenesis. The mutation introduced, proline-25 to glutamine, is in close proximity to the arginine-47 residue thought to be responsible for the initial docking of fatty acid substrates. The P25Q mutant displays an affinity for palmitate which is approximately 100-fold weaker than the wild-type enzyme. In addition to its altered substrate affinity, P25Q also exhibits altered hydroxylation specificity and carbon monoxide recombination kinetics in the substrate-free form.

© 1997 Federation of European Biochemical Societies.

**Key words:** Random mutagenesis; Substrate binding; Regiospecificity; Carbon monoxide geminate kinetics

## 1. Introduction

Cytochrome P450<sub>BM-3</sub> is a heme-containing monooxygenase isolated from *Bacillus megaterium* and is one of only two known P450s that are catalytically self-sufficient [1,2]. They consist of a single polypeptide containing both a catalytic heme domain and a FAD/FMN reductase domain which utilizes NADPH as an electron donor. P450<sub>BM-3</sub> catalyzes the  $\omega$ - $n$  ( $n=1-3$ ) hydroxylation of fatty acids of varying chain lengths [3]. The proposed mechanism for this reaction begins with substrate binding and proceeds through a number of intermediates which result in oxidation of the substrate and regeneration of the resting state of P450. In P450<sub>cam</sub>, where much of the cytochrome P450 mechanism has been elucidated [4], the initial binding of substrate in the active-site pocket replaces a water molecule ligated to the heme and results in a change from a low-spin six-coordinated iron to a high-spin five-coordinated iron [5–7]. A similar reaction cycle is thought to be operational in P450<sub>BM-3</sub>.

The crystal structure of P450<sub>cam</sub> shows a largely hydrophobic heme pocket with no clear access channel for the substrate [8]. In comparison, the active site of P450<sub>BM-3</sub> appears very different, with the presence of a long predominately hydrophobic channel providing a clear path for the substrate to the heme [9]. Another interesting difference between the two active sites is the observation that P450<sub>BM-3</sub> appears to undergo a large-scale conformational change following substrate bind-

ing. While this conformation change is not yet fully understood, recent work including dynamic simulations [10], solution of the substrate-bound crystal structure [11] and carbon monoxide (CO) recombination kinetics [12] demonstrate a large difference between the substrate-bound and substrate-free forms, suggesting a closing or occlusion of the active site upon binding. In addition, the substrate-bound crystal structure shows that the substrate initially binds at a distance of approximately 7 Å from the iron. NMR paramagnetic relaxation studies suggest that the substrate then undergoes physical displacement upon reduction of the enzyme, bringing the substrate closer to the iron [13].

The initial docking of fatty acid substrates is thought to be mediated by the formation of hydrogen bonds or ion pairs between the carboxylic acid group of the substrate and residues Arg<sup>47</sup> and Tyr<sup>51</sup> [11,14]. Replacement of R47 with a negatively charged residue inhibited catalysis completely, while mutation to an alanine allowed for substrate turnover, but led to a decreased affinity for substrate and an altered product distribution [14]. These results suggested that R47 is responsible for the initial tight binding and subsequent orientation of the substrate in the active site.

Several other studies utilized site-directed mutagenesis to elucidate interactions important for molecular recognition in P450<sub>BM-3</sub> [15–18]. While these studies have greatly contributed to our current understanding of substrate binding, there are limitations of how much information one can obtain in a given time period using these methods. Instead, another approach to the problem is to first seek an interesting substrate-binding phenotype, and then determine the molecular basis for the change in specificity, which can be accomplished by generating a large library of mutants via random mutagenesis. One advantage of this method is the ability to discover mutations perturbing important interactions which may not have otherwise been predicted.

In this communication, the results from random mutagenesis of P450<sub>BM-3</sub> will be discussed. As a result of this work the mutation P25Q, which is located in the substrate access channel, was found to greatly reduce the binding affinity of palmitate to the enzyme. This mutation is not located in any of the proposed substrate recognition regions [19], and therefore would probably not have been otherwise predicted to affect substrate binding. Hence, random mutagenesis methods can uncover important structural features in cytochrome P450 that determine substrate specificity, even those that are distant from the heme active center and/or may not be obvious from the static crystal structure.

## 2. Material and methods

The library of random P450<sub>BM-3</sub> mutants was generated by trans-

\*Corresponding author. Fax: (217) 244-7100

<sup>1</sup>Present address: Doping Control Center, Korea Institute of Science and Technology, Seoul, Korea.

This work was supported by grants (GM 33775 and GM 31756) from the National Institute of Health.

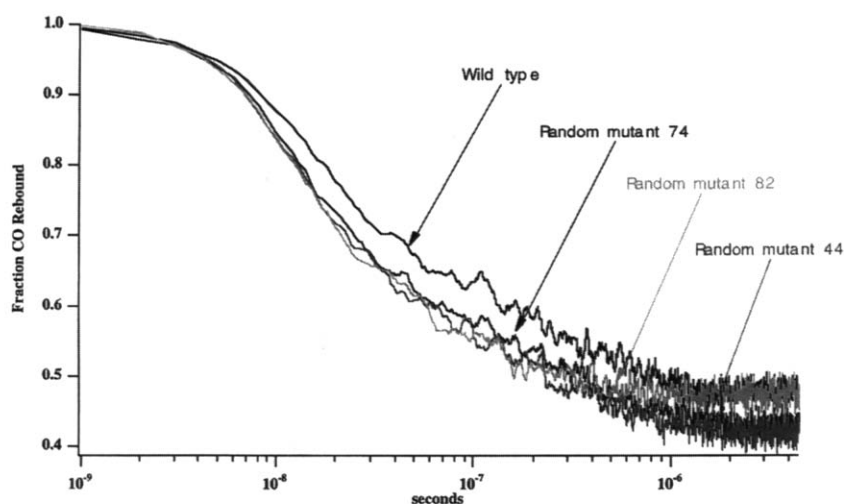


Fig. 1. Geminate CO rebinding transients for wild-type P450<sub>BM-3</sub> and random mutants 44, 74, and 82. The traces were measured using lysate solutions of the protein to give ODs of 0.01. 300 averages were taken of each sample and all were normalized to the maximum absorbance change.

forming the pUC13bm3 [20] plasmid containing the *P450* gene into an *E. coli* mutator strain, XL1-Red® from Stratagene. This mutator strain is deficient in its ability to repair mismatches through the 3' to 5' exonuclease activity of DNA polymerase III, and its ability to hydrolyze 8-oxodGTP. Stratagene reports an average mutation rate of one mutation per every 2000 nucleotides per colony [20]. While the entire plasmid contains 7.65 kb, only mutations made in the 1.41 kb heme domain coding region should have an effect on substrate binding. Therefore, one could expect to see an average of 3–4 mutations in each colony, with only 0–1 mutations per colony in the heme domain region. Plasmid DNA was extracted from 91 of the 100 cultures and purified by alkaline lysis of the cell pellet [21]. Each purified plasmid DNA was then transformed into competent DH5- $\alpha$  cells to keep the DNA stable and prevent further mutations.

### 2.1. Screening the library

Cell lysate solutions of the random mutants were used for all of the screening. These were prepared from 50 ml cell cultures for each random mutant. The cell pellets were resuspended in 0.6 ml of lysis buffer (50 mM potassium phosphate, pH 8.0, 0.1 mM EDTA, 8 mM MgCl<sub>2</sub> and 2 mM dithiothreitol (DTT)) and lysed by sonication for two 30 s periods interspersed by a 1 min incubation on ice.

Expression levels of P450<sub>BM-3</sub> in each colony were determined by CO difference spectra [22]. The electronic absorbance spectra were obtained with a Hitachi U-3300 spectrometer using a scan rate of 600 nm/min.

The library was then screened by comparing CO geminate recombination kinetics using flash photolysis. The samples contained enough P450<sub>BM-3</sub> lysate solution (100–200  $\mu$ l) to give a total optical density change of roughly 0.01 in the geminate traces, 200  $\mu$ M sodium laurate, and dithionite in 0.1 M potassium phosphate buffer (pH 7.4) saturated with CO. The CO geminate kinetics for the purified proteins were taken with concentrations of 2.5  $\mu$ M P450 and 100  $\mu$ M palmitate.

The laser flash photolysis system utilized for these investigations has been previously described [12]. Data was taken on the microsecond time scale with the monochromator passband at 450 nm with a 3–4 nm width. The data was analyzed using Mathematica (Wolfram Re-

search). All spectra were normalized to unity by the maximum observed change in optical density.

### 2.2. Protein purification and characterization

The three random P450<sub>BM-3</sub> mutants selected for further screening were over expressed in *E. coli* and purified to homogeneity. Each mutant was purified in the same manner as wild type, as previously described in the literature [23].

The mass spectra of the proteins were obtained at the Mass Spectrometry Laboratory at the University of Illinois, using the electrospray ionization technique with a VG Quattro mass spectrometer. DNA sequencing of puc13bm3r82 plasmid DNA was accomplished by both dideoxy chain termination method (USB) and fluorescence labeling at the University of Illinois Sequencing Facility.

Product distribution analysis for the fatty acid hydroxylations was carried out as previously described [24]. The xanthotoxin metabolism assays were carried out as previously described [25] and analyzed by HPLC. The reactions used protein concentrations ranging from 0.9 to 2.5  $\mu$ M. The rate of NADPH oxidation was measured by monitoring the decrease in absorbance at 340 nm using an extinction coefficient of 6.22 mM<sup>-1</sup> cm<sup>-1</sup>. The reaction consisted of 0.1 M potassium phosphate, pH 8.0, 200  $\mu$ M substrate and varying amount of protein, and was initiated with 150  $\mu$ M NADPH. The oxidation rate was calculated from the rate over the first 30 s.

Substrate binding was measured by spectrophotometric titration of protein with substrate at 25°C. The reaction mixture contained 1–2  $\mu$ M enzyme in 0.5 M KPi, pH 8.3. Binding of substrate induced a spin state change from low to high spin with Soret band shift from 418 to 392 nm. The dissociation constant was determined from the slope of the plot  $(\Delta A_{418} + \Delta A_{392})$  versus  $(\Delta A_{418} + \Delta A_{392})/[\text{substrate}]$ .

### 2.3. Molecular modeling of P25Q

Using the crystal structure of wild-type substrate-bound P450<sub>BM-3</sub> [11], the mutation found in random mutant 82 (P25Q) was modeled using QUANTA (MSI) molecular graphics and modeling software. The residue Pro<sup>25</sup> was replaced with a glutamine and then the protein was energy minimized using the CHARMm package with the steepest descent method, while constraining the heme atoms.

Table 1  
Regiospecificity for fatty acid hydroxylation of wild-type (WT) BM3 and P25Q mutant

Hydroxylated position	Laurate (%)		Myristate (%)		Palmitate (%)	
	WT	P25Q	WT	P25Q	WT	P25Q
$\omega$ -1	35 $\pm$ 0.7	31.5 $\pm$ 0.5	44.5 $\pm$ 2.2	35.0 $\pm$ 1.6	34 $\pm$ 1.8	25 $\pm$ 2.6
$\omega$ -2	29 $\pm$ 0.8	28.5 $\pm$ 0.6	34.0 $\pm$ 2.8	27.5 $\pm$ 1.9	46 $\pm$ 1.7	50 $\pm$ 0.8
$\omega$ -3	36 $\pm$ 0.7	40.0 $\pm$ 0.5	21.5 $\pm$ 3.5	37.5 $\pm$ 2.6	20 $\pm$ 0.9	25 $\pm$ 2.3

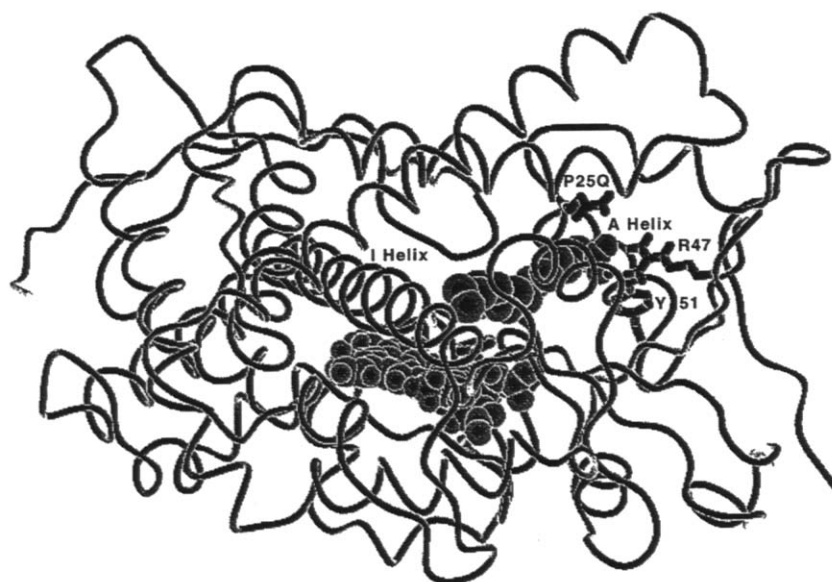


Fig. 2. Energy minimized model structure of P450<sub>BM-3</sub> with the P25Q mutation replaced in the crystal structure of the palmitoleic bound P450<sub>BM-3</sub> [11]. The spatial relation of residues Y51 and R47 to the P25Q mutation are shown, as well as the palmitoleic substrate and the heme group.

### 3. Results

The CO difference spectra of the random library show a wide range of expression levels for the mutant P450<sub>BM-3</sub> proteins. Although the expression of each mutant varied slightly each time it was grown, some mutants consistently expressed better than others. One mutant culture showed a small Soret peak at 420 nm instead of 450 nm which is characteristic of expression of the inactive form of the enzyme, cytochrome P420.

Screening by CO flash photolysis produced three mutants with significantly different geminate rates than the wild type. Most of the geminate recombination kinetics of the mutants were identical to that of wild type within the sensitivity of these measurements. Fig. 1 displays the CO geminate transients of wild-type and random mutants 44, 74, and 82. These three were selected as qualitatively having different transients than the wild-type protein.

Mass spectrometry data was obtained for wild-type and random mutants 82 and 74. The mass of mutant 82 ( $117685 \pm 20$  Da) is consistent with a single point mutation when compared to the wild type ( $117643 \pm 26$  Da). The mass of mutant 74 (56000 Da) suggested a truncation of the protein and was therefore excluded from further characterizations. The mass of mutant 44 was consistent with that of wild type.

Table 1 presents the data for the relative product distributions of the  $\omega$ -1,  $\omega$ -2 and  $\omega$ -3 hydroxylation products for wild-type and the P25Q mutant (random mutant 82). The

distributions for random mutant 44 were approximately  $\pm 2\%$  the values of wild type (data not shown).

The mutants were assayed for xanthotoxin metabolism in order to assay for changes in the binding pocket which would enhance the catalysis of a non-native substrate. The results show a decrease in activity for mutant 82 as compared to wild type. Although the activity of P450<sub>BM-3</sub> is overall much less for xanthotoxin than its natural fatty acid substrates, it is drastically reduced in mutant 82. The specific activity of xanthotoxin for wild-type, mutant 44, and mutant 82 were  $19.2 \pm 0.2$ ,  $16.8 \pm 0.8$ , and  $1.5 \pm 0.03$  fmol Xanthotoxin  $\text{min}^{-1}$  pmol P450<sup>-1</sup>, respectively. Since both the fatty acid product distributions and the xanthotoxin activity for mutant 44 were similar to wild type, it was excluded from further characterization.

The sequence for random mutant 82 heme domain showed only a single mutation of a cytosine to adenine. The resulting protein mutation was the change of amino acid number 25 from a proline to a glutamine. A model of the minimized structure of P25Q P450<sub>BM-3</sub> is shown in Fig. 2. This modeled structure shows the proximity of the P25Q mutation, residue R47, and residue Y51 relative to the substrate and heme.

The NADPH oxidation rates for P25Q P450<sub>BM-3</sub> and experimental dissociation constants are presented in Table 2. Typical plots for the determination of dissociation constants for wild type and P25Q are shown in Fig. 3. The dissociation constants show only a small difference in values for laurate, approximately a 5-fold change for the binding of myristate to the P25Q mutant, and approximately a 125-fold change in the

Table 2  
NADPH oxidation rates and substrate dissociation rates for wild-type (WT) and P25Q P450<sub>BM-3</sub>

Substrates	NADPH oxidation (nmol/min/nmol P450)		Dissociation constant ( $\mu\text{M}$ )	
	WT	P25Q	WT	P25Q
Laurate	$893 \pm 50$	$434 \pm 76$	$27.20 \pm 5.0$	$34.4 \pm 1.0$
Myristate	$2461 \pm 156$	$1558 \pm 89$	$2.17 \pm 0.3$	$10.9 \pm 0.28$
Palmitate	$2360 \pm 172$	$2012 \pm 135$	$0.021 \pm 0.005$	$2.87 \pm 0.6$

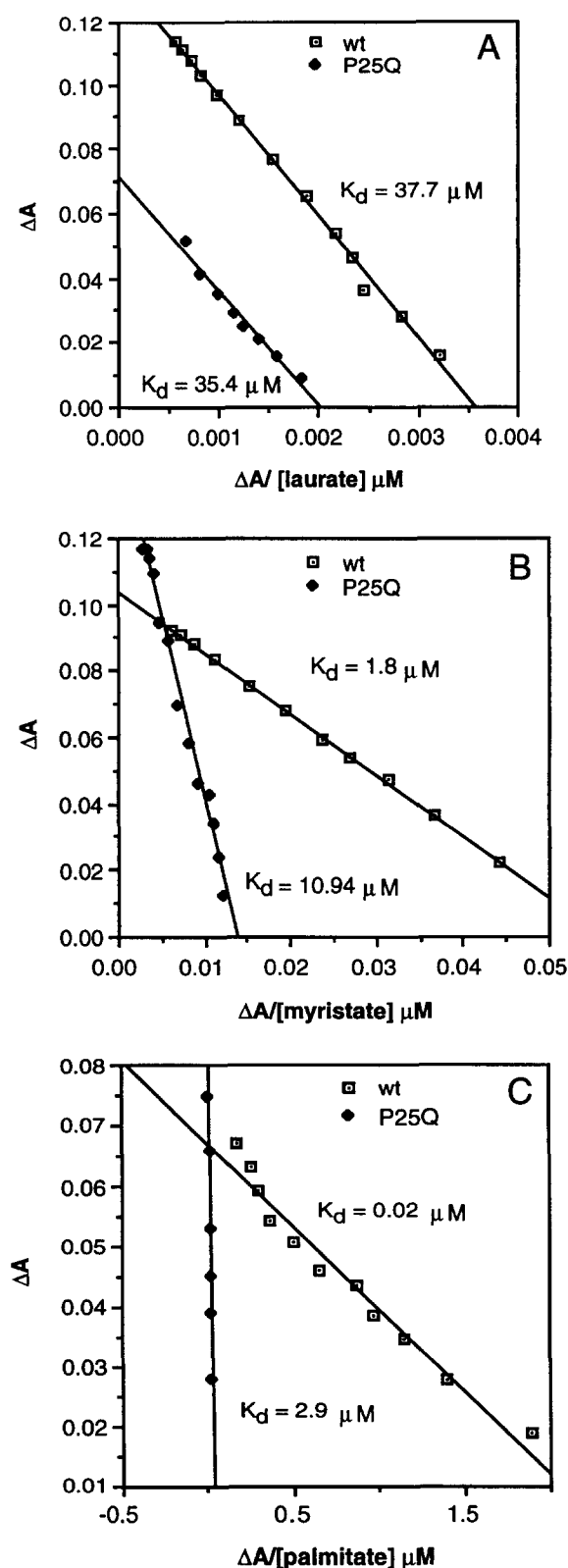


Fig. 3. An Eadie-Hofstee like plot for the determination of substrate dissociation constants for the wild type and P25Q for three fatty acid substrates. (A) laurate, (B) myristate, (C) palmitate.

binding of palmitate. It should be noted that the values determined cannot be compared to those previously published [26,27], since these experiments were conducted at a higher pH

(pH 8.3) to increase the solubility of the fatty acids. Also, to alleviate the need to reach a saturated endpoint for the determination of the concentration of free substrate, an Eadie-Hofstee like plot was used, where  $\Delta A$  versus  $\Delta A/[substrate]$  was plotted. From this plot, the dissociation constant is determined from the slope and  $\Delta A_{max}$  is extrapolated. This allows for the determination of dissociation constants without having to reach a saturated endpoint. The data was replicated several times for each sample and was found to be reproducible by this method.

CO geminate recombination rates were determined for the purified P25Q and wild-type proteins. The data was fitted with a four-state sequential model, as proposed in previous work [12]. The geminate rate constants and yields are given in Table 3. The kinetics for P25Q appear to be about the same as wild type. There is no difference in the geminate yields of substrate-bound P25Q and wild type; however, the substrate-free form of P25Q has a 5% lower geminate yield than the wild type. These results are consistent at both low (100 mM KPi) and high (250 mM KPi) salt concentrations.

#### 4. Discussion

Over the last several years many studies have contributed to better understanding the substrate-binding process in P450 enzymes. The focus has primarily been on using crystal structures [11,28], sequence alignments [19,29], and experimental data to help predict what changes a particular mutation should induce on substrate metabolite profiles. While headway has been made in this area, there are still a lot of questions which remain unanswered. In this communication we have used random mutagenesis to shed light on important residues controlling substrate binding and metabolism in P450<sub>BM-3</sub>.

While the methodologies associated with random mutagenesis can generate large libraries with a potential spectrum of alterations in enzymatic function, the high degeneracy requires creative solutions to the problems of screening. The method of screening successful in this case was the use of CO geminate recombination in a similar manner to one previously used by Huang and Boxer [30]. CO geminate rebinding has previously provided substantial information about ligand binding and conformational dynamics for various cytochrome P450s [31–33]. Most recently, a study on CO binding in P450<sub>BM-3</sub> has provided important information on the conformational dynamics of this heme protein [12]. This study showed large changes in the recombination kinetic rate constants between the substrate-bound and substrate-free forms of the native protein. Therefore, it was postulated that alterations in the substrate-binding pocket should be detectable by observing changes in the CO recombination kinetics. This method afforded the two major advantages of being protein concentration independent and a sensitive probe of the P450 active site.

Screening by CO geminate recombination produced three possible candidates which had qualitatively different kinetic rates than the wild type. Upon further characterization of these three random mutants, one mutant P450 was found to have drastically different substrate-binding properties. The data from mass spectrometry, fatty acid product analysis, and xanthotoxin metabolism aided in narrowing down these few mutants. The selected mutant, P25Q, had different char-

Table 3  
CO geminate rates for wild type and P25Q

$\text{Fe-CO} \xrightleftharpoons[k_1]{h\nu} \text{Fe::CO} \xrightleftharpoons[k_3]{k_2} \text{Fe:::CO} \xrightleftharpoons[k_5]{k_4} \text{Fe} + \text{CO}$					
	$k_1$ ( $\mu\text{s}^{-1}$ )	$k_2$ ( $\mu\text{s}^{-1}$ )	$k_3$ ( $\mu\text{s}^{-1}$ )	$k_4$ ( $\mu\text{s}^{-1}$ )	Gem. yield (%)
Substrate free					
WT	$9.3 \pm 0.5$	$40.3 \pm 1.0$	$1.6 \pm 0.2$	$4.7 \pm 0.2$	20
P25Q	$8.8 \pm 0.4$	$51.2 \pm 1.0$	$0.95 \pm 0.09$	$4.8 \pm 0.6$	15
Palmitate bound					
WT	$20.1 \pm 1.2$	$25.7 \pm 3.6$	$3.2 \pm 0.6$	$5.1 \pm 0.1$	53
P25Q	$20.8 \pm 0.2$	$30.3 \pm 0.2$	$3.7 \pm 0.5$	$6.2 \pm 0.2$	52

acteristics than wild type in all of these assays, again indicating a perturbation of the active site.

Molecular modeling of P25Q P450<sub>BM-3</sub>, together with the help of the recently solved crystal structure for palmitoleic-bound P450<sub>BM-3</sub> [11], provided substantial insight as to the origin of the altered specificities. The substrate access channel is fairly open in the substrate-free crystal form, placing P25 a significant distance from the substrate. However, in the substrate-bound crystal form, P25 is directly across from the R47 and T51 residues which are thought to be involved in forming ionic bonds or hydrogen bonding to the carboxyl end of the substrate. The modeled structure of the P25Q mutant shows a significant steric hindrance of the substrate due to the extension of the glutamine side chain. It is also possible that a glutamine residue in this position could hydrogen bond to the carboxyl group on the substrate, conceivably causing the substrate to orient differently in the pocket.

Detailed characterization of the P25Q mutation revealed three main effects of the mutation, consistent with the proposed model. The largest effect was a 100-fold decrease in affinity for palmitate. This represents a significant change in the active site to accommodate the C-16 fatty acid. The effect drastically decreased as the size of the fatty acid decreased. This is most likely due to the tighter fit of the longer chain fatty acids in the binding pocket as opposed to the 'looser' fitting of the shorter chains. Since Arg<sup>47</sup> has been suggested to provide interactions necessary for the initial docking of the substrate, it follows that a large steric hindrance in close proximity would greatly decrease the affinity for the substrate, especially the tighter fitting substrates.

The second effect was a change in distribution of the hydroxylation products by P25Q. For the three substrates, the trend is a change in preference for hydroxylation from  $\omega$ -1 to  $\omega$ -3. These changes in hydroxylation specificity of the enzyme can be explained by a different orientation of the substrate in the pocket of P25Q. The terminal end of the substrate is perhaps being oriented in a slightly different position, to accommodate for the steric hindrance and the possible formation of new hydrogen bonds to the glutamine residue at the carboxy end of the substrate.

The third observed effect was alteration of the CO geminate recombination kinetics of the purified protein. The P25Q mutation shows no noticeable effect on the substrate-bound form of the protein, but lowers the geminate yield of the substrate-free form. If the P25Q mutation is predominately causing a steric hindrance in the substrate access channel, it could be

rationalized as closing the pocket and therefore, having a slightly higher geminate yield. However, since in the substrate-free form it is causing a decrease in geminate yield, there is clearly another effect contributing. It is possible that the glutamine residue induces changes on the structure of the A helix. Residue 25 is the first residue of the A helix of P450<sub>BM-3</sub>, which lies near the top of the substrate access channel. If this structure were slightly altered due to the differences of phi-psi angles between proline and glutamine, the helix could shift and result in a more open conformation of the access channel. Then upon substrate binding, the interactions between the substrate and protein in this area would force the helix back into the 'wild type' orientation, and afford CO rebinding kinetics similar to wild type.

Results obtained from the steady-state turnover show only small differences between wild type and P25Q. Although P25Q binds palmitate approximately 100-fold weaker than wild type, the maximal velocities of NADPH oxidation were approximately the same. Therefore, this residue does not appear to play a large role in the catalytic mechanism, rather the differences seem to be caused by alterations in substrate recognition and orientation.

In summary, a mutation in the region that is thought to be responsible for initial recognition of the fatty acids, has been isolated where the affinity of the tightly binding substrates and the regioselectivity for hydroxylation is greatly reduced. This can be attributed to both steric hindrance and a possible conformation change of the protein in the substrate-free form. Through the use of random mutagenesis we were able to elucidate an interesting mutation which provides information about the initial recognition and docking of substrate, which may not have otherwise been found.

**Acknowledgements:** We thank Dr. Mary Schuler and Dr. Eric Chien for their expert assistance with the xanthotoxin assays and all of their insightful input in the initial stages. We also thank Dr. Thomas Poulos for giving us the palmitoleic-bound P450<sub>BM-3</sub> crystal structure coordinates and helpful interpretations of that structure. We thank Aretta Weber for her excellent editorial assistance.

## References

- [1] Narhi, L.O. and Fulco, A.J. (1986) *J. Biol. Chem.* 261, 7160–7169.
- [2] Nakayama, N., Takemae, A. and Shoun, H. (1996) *J. Biochem.* 119, 435–440.
- [3] Miura, Y. and Fulco, A.J. (1975) *Biochim. Biophys. Acta* 388, 305–317.

- [4] E.J. Mueller, P.J. Loida, and S.G. Sligar, in: P.R. Ortiz de Montellano (Ed.), *Cytochrome P450 Structure, Mechanism, Biochemistry*, Plenum Press, New York, 1995, pp. 83–124.
- [5] Sligar, S.G. (1976) *Biochemistry* 15, 5399–5406.
- [6] Sligar, S.G., Cinti, D.L., Gibson, G.G. and Schenkman, J.B. (1979) *Biochem. Biophys. Res. Commun.* 90, 925–932.
- [7] Fisher, M.T. and Sligar, S.G. (1985) *J. Am. Chem. Soc.* 107, 5018–5019.
- [8] Poulos, T.L., Finzel, B.C. and Howard, A.J. (1987) *J. Mol. Biol.* 195, 687–700.
- [9] Ravichandran, K.G., Bouddupalli, S.S., Hasemann, C.A., Peterson, J.A. and Deisenhofer, J. (1993) *Science* 261, 731–736.
- [10] Paulsen, M.D. and Ornstein, R.L. (1995) *Prot. Struct. Funct. Genet.* 21, 237–243.
- [11] Li, H. and Poulos, T. (1997) *Nature Struct. Biol.* 4, 140–146.
- [12] Mclean, M.A., Yeom, H. and Sligar, S.G. (1996) *Biochimie* 78, 700–705.
- [13] Modi, S., Sutcliffe, M.J., Primrose, W.U., Lian, L.-Y. and Roberts, G.C.K. (1996) *Nature Struct. Biol.* 3, 414–417.
- [14] Graham-Lorence, S., Truan, G., Peterson, J.A., Falck, J.R., Wei, S., Helvig, C. and Capdevila, J.H. (1997) *J. Biol. Chem.* 272, 1127–1135.
- [15] Porter, T.D. (1994) *Biochem.* 33, 5942–5946.
- [16] J.A. Peterson and S.E. Grahm-Lorence, in: P.R. Ortiz de Montellano (Ed.), *Cytochrome P450, Structure, Mechanism, and Biochemistry*, Plenum Press, New York, 1995, pp. 151–180.
- [17] Imai, Y. and Nakamura, M. (1989) *Biochem. Biophys. Res. Commun.* 158, 717–722.
- [18] Oliver, C.F., Modi, S., Sutcliffe, M.J., Primrose, W.U., Lias, L.-Y. and Roberts, G.C.K. (1997) *Biochemistry* 36, 1567–1572.
- [19] Gotoh, O. (1992) *J. Biol. Chem.* 267, 83–90.
- [20] Stratagene, Epicurian Coli® XL1-Red Competent Cells Instruction Manual, 1994.
- [21] T. Maniatis, E.F. Fritsch, and J. Sambrook, *Molecular Cloning: A Laboratory Manual*, Cold Spring Harbor Laboratory Press, Cold Spring Harbor, NY, 1989.
- [22] Omura, T. and Sato, R. (1964) *J. Biol. Chem.* 239, 2370–2378.
- [23] Yeom, H., Sligar, S.G., Li, H., Poulos, T.L. and Fulco, A.J. (1995) *Biochemistry* 34, 14733–14740.
- [24] Yeom, H. and Sligar, S.G. (1997) *Arch. Biochem. Biophys.* 337, 209–216.
- [25] Ma, R., Cohen, M., Berenbaum, M.R. and Schuler, M.A. (1994) *Arch. Biochem. Biophys.* 310, 332–340.
- [26] Modi, S., Primrose, W., Boyle, J.M.B., Gibson, C.F., Lian, L.-Y. and Roberts, G.C.K. (1995) *Biochemistry* 34, 8982–8988.
- [27] Shanthi, G. and Poulos, T.L. (1995) *Biochemistry* 34, 11221–11226.
- [28] Li, H. and Poulos, T.L. (1995) *Acta Cryst. D51*, 21–32.
- [29] Hasemann, C.A., Kurumbail, R.G., Boddupalli, S.S., Peterson, J.A. and Deisenhofer, J. (1995) *Structure* 3, 41–62.
- [30] Huang, X. and Boxer, S.G. (1994) *Nature Struct. Biol.* 1, 226–229.
- [31] Unno, M., Ishimori, K., Ishimura, Y. and Morishima, I. (1994) *Biochemistry* 33, 9762–9768.
- [32] Tian, W.D., Wells, A.V., Champion, P.M., Di Primo, C., Gerber, N. and Sligar, S. (1995) *J. Biol. Chem.* 270, 8673–8679.
- [33] Koley, A.P., Buters, J.T.M., Robinson, R.C., Markowitz, A. and Friedman, F.K. (1995) *J. Biol. Chem.* 270, 5014–5018.